

A new quasi-one-dimensional molecular solid based on Ni(mnt)₂ anion: Crystal structure and spin–gap transition

Chunlin Ni*, Xiaoping Liu, Linliang Yu, Leming Yang

Department of Applied Chemistry, Centre of Inorganic Functional Materials, College of Science, South China Agricultural University, 510642 Guangzhou, PR China

Received 22 June 2006; received in revised form 23 August 2006; accepted 8 September 2006

Abstract

A new molecular solid, [1-(4'-bromo-2'-fluorobenzyl)-4-dimethylaminopyridinium]-bis(maleonitriledithiolato)nickel(III), (BrFBzPyN(CH₃)₂)(Ni(mnt)₂)(**1**), has been prepared and characterized by elemental analyses, IR, ESI-MS spectra, single crystal X-ray diffraction and magnetic measurements. Compound **1** crystallizes in the orthorhombic space group Pnma, $a = 20.579(4) \text{ \AA}$, $b = 7.078(1) \text{ \AA}$, $c = 17.942(4) \text{ \AA}$, $\alpha = \beta = \gamma = 90^\circ$, $V = 2613.3(9) \text{ \AA}^3$, $Z = 4$. The Ni(III) ions of **1** form a quasi-one-dimensional Zigzag magnetic chain within a Ni(mnt)₂[−] column through Ni⋯S, S⋯S, Ni⋯Ni, or $\pi \cdots \pi$ interactions with an Ni⋯Ni distance of 4.227 Å. Magnetic susceptibility measurements in the temperature range 2–300 K show that **1** exhibits a spin–gap transition around 200 K, and antiferromagnetic interaction in the high-temperature phase (HT) and spin gap in the low-temperature phase (LT). The transition for **1** is second-order phase transition as determined by DSC analyses.

© 2006 Elsevier Ltd. All rights reserved.

Keywords: A. Magnetic materials; D. Crystal structure; D. Magnetic properties

1. Introduction

Molecular solids based on transition metal dithiolene complexes have attracted intense interest in recent years, not only owing to the fundamental research of magnetic interactions and magneto-structural correlations but also to the development of new functional molecule-based materials [1]. Much work has been performed in molecular solids based on [M(mnt)₂][−] (mnt^{2−} = maleonitriledithiolate, M = Ni(III) or Pt(III)) ions owing to their application as building blocks in molecular-based materials showing magnetic, superconducting, and optical properties [2–8]. Especially, the discovery in 1996 of the ferromagnetic complex containing Ni(mnt)₂[−] ion, NH₄·Ni(mnt)₂·H₂O, strongly stimulated the study on Ni(mnt)₂ complexes as building blocks for new molecular magnets [9]. The emphasis on synthesizing these molecular solids is to search for suitable multifunctional organic cations such as substituted

benzylpyridinium derivatives as the counteraction that can effectively mediate the magnetic coupling between the spin carriers [Ni(mnt)₂] anions, and establish a relationship between the magnetic interactions and the stacking pattern of anions or cations [10–15]. Recently, we reported the preparation, crystal structure and magnetic properties of a new ion-pair complex, [BrFBzPyNH₂][Ni(mnt)₂] [BrFBzPyNH₂⁺ = 1-(4'-bromo-2'-fluorobenzyl)-4-aminopyridinium] that exhibits interesting magnetic properties: the occurrence of significant ferromagnetic interaction in the high-temperature phase (HT), spin–gap transition in the low-temperature phase (LT) and weak ferromagnetism due to spin canting below 5 K [16]. With a view to obtaining molecular solid with novel properties and to investigate methyl groups in amino group of 4-aminopyridine, we selected organic cation [BrFBzPyN(CH₃)₂]⁺ to tune the crystal stacking structure of [M(mnt)₂] anion, and obtained a new quasi-one-dimensional molecular solid, (1-(4'-bromo-2'-fluorobenzyl)-4-dimethylaminopyridinium)-bis(maleonitriledithiolato)nickel, [BrFBzPyN(CH₃)₂][Ni(mnt)₂](**1**) showing a spin–gap transition around 200 K and a spin gap below this temperature. To the best of our knowledge, the

*Corresponding author. Fax: +86 20 85282366.

E-mail address: niclchem@scau.edu.cn (C. Ni).

1D chain exhibiting a spin–gap transition above 200 K is very rare for the Ni(mnt)₂ complexes.

2. Experimental

2.1. Synthesis

The starting materials were commercial 4'-bromo-2'-fluorobenzyl bromide (Fluka, 98%) and 4-dimethylaminopyridine (Aldrich, 99%). 1-(4'-bromo-2'-fluorobenzyl)-4-dimethylaminopyridinium bromide and disodium maleonitriledithiolate (Na₂mnt) were synthesized following the published procedures [17,18]. (1-(4'-bromo-2'-fluorobenzyl)-4-dimethylaminopyridinium)₂[Ni(mnt)₂] was prepared by the direct combination of 1:2:2 mol equiv of NiCl₂·6H₂O, Na₂mnt and 1-(4'-bromo-2'-fluorobenzyl)-4-dimethylaminopyridinium bromide in water by a similar method described in the literature [18]. (1-(4'-Bromo-2'-fluorobenzyl)-4-dimethylaminopyridinium)₂[Ni(mnt)₂] (960 mg, 1.0 mmol) was dissolved in 60 ml MeCN, then a MeCN solution (10 ml) of I₂ (180 mg, 0.71 mmol) was slowly added, the mixture was stirred for 4 h, and then 80 ml MeOH was added. After the mixture was allowed to stand overnight, 556 mg dark microcrystals produced were filtered off, washed with MeOH and Et₂O and dried in a vacuum. Single crystals suitable for X-ray structure analyses were obtained by evaporating solution of **1** in mixtures of MeCN and *i*-PrOH (1:2 v/v). Yield: 85.7%. *Anal.* Calc. for C₂₂H₁₅BrFN₆NiS₄: C, 40.70; H, 2.33; N, 12.94; Ni, 9.04%. Found: C, 40.58; H, 2.47; N, 12.82; Ni, 8.97%. IR (cm⁻¹): 2208.9 s, ν(CN); 1487.8 s, ν(C=C) of mnt²⁻. ESI-MS (MeCN): 340.1, [Ni(mnt)₂+H]⁻; 310.2, [BrFBzPyN(CH₃)₂]⁺.

2.2. Physical measurements

The elemental analyses (C, H, and N contents) were performed on a Model 240 Perkin Elmer C H N instrument. Nickel content was determined using a Varian 220FS/220Z atomic absorption spectrophotometer. An infrared spectrum was collected on an IF66 V FT-IR (400–4000 cm⁻¹ region) spectrophotometer using KBr pellets of the samples. DSC was carried out with a Perkin–Elmer calorimeter, and thermal analysis of crushed polycrystalline sample for **1** placed in an aluminum crucible was performed on warming (rate of 20 K min⁻¹) from 100 to 300 K. Magnetic susceptibilities data on crushed polycrystalline sample of **1** were collected over the temperature range 2.0–300 K using a Quantum Design MPMS-5S super-conducting quantum interference device (SQUID) magnetometer, and the experimental data were corrected for diamagnetism of the constituent atoms estimated from Pascal's constants.

2.3. Determination of crystal structure

The intensity data of the Ni(III) complex **1** were collected using a Siemens SMART CCD area detector (Mo–K α radiation, $\lambda = 0.71073$ Å) at 293 K. The structure was solved by direct method using SHELXS 97 and refined

on F^2 by full-matrix least-squares methods (SHELXL 97) [19]. All the non-hydrogen atoms were easily found from Fourier map and refined anisotropically. Hydrogen atoms were constrained to ride on the respective carbon atoms with an isotropic displacement parameter equal to 1.2 times the equivalent isotropic displacement parameter of their parent atom. The details of data collection, refinement and crystallographic data are summarized in Table 1.

3. Results and discussion

3.1. Crystal structure

The molecular structure of **1** with non-hydrogen atomic labeling in an asymmetric unit is shown in Fig. 1a. An asymmetric unit in a cell comprises an ion pair of [Ni(mnt)₂]⁻ and [BrFBzPyN(CH₃)₂]⁺. The Ni(III) ion in the [Ni(mnt)₂]⁻ anion is coordinated by four sulfur atoms of two mnt²⁻ ligands, and exhibits square-planar coordination geometry. All atoms of [Ni(mnt)₂]⁻ anion are in a plane and the bond lengths and angles within the anion are in fair agreement with those of [BrFBzPyNH₂][Ni(mnt)₂] [16]. Selected bond distances, bond angles, and intermolecular Ni...Ni, Ni...S, and S...S distances of **1** are summarized in Table 2. In the [BrFBzPyN(CH₃)₂]⁺ moiety, the C14–C15–N5 reference plane shares a plane with the benzene ring, which is completely perpendicular to the pyridine ring. Both anions and cations form segregated stacks whose directions are parallel to the *b*-axis as shown in Fig. 1b. Face-to-face overlap (Fig. 2a) involves an anionic pair containing Ni(I) and Ni(1A) (symmetric code $A = 3/2 - x, -y, 3/2 + z$), in which the distance between the

Table 1
Crystallographic data for **1**

Temperature (K)	293(2)
Empirical formula	C ₂₂ H ₁₅ BrFN ₆ NiS ₄
Crystal size (mm)	0.45 × 0.38 × 0.30
Space system	Orthorhombic
Formula weight	649.27
Space group	Pnma
Unit cell dimensions	
<i>a</i> (Å)	20.579(4)
<i>b</i> (Å)	7.078(1)
<i>c</i> (Å)	17.942(4)
Volume (Å ³), <i>Z</i>	2613.3(9), 4
Density (g cm ⁻³)	1.650
λ (Å)	0.71073
2θ range (°)	3.96 < 2θ < 50.0
μ (Mo K α)(mm ⁻¹)	2.622
Reflection collected	12628
Unique reflection, R_{int}	2508, 0.080
Goodness of fit on F^2	1.008
Observed data [$I > 2\sigma(I)$]	1783
R_1	0.0362, 0.0580
wR_2	0.0686, 0.0730
Largest diff peak and hole (e ⁻ Å ⁻³)	0.45, -0.39

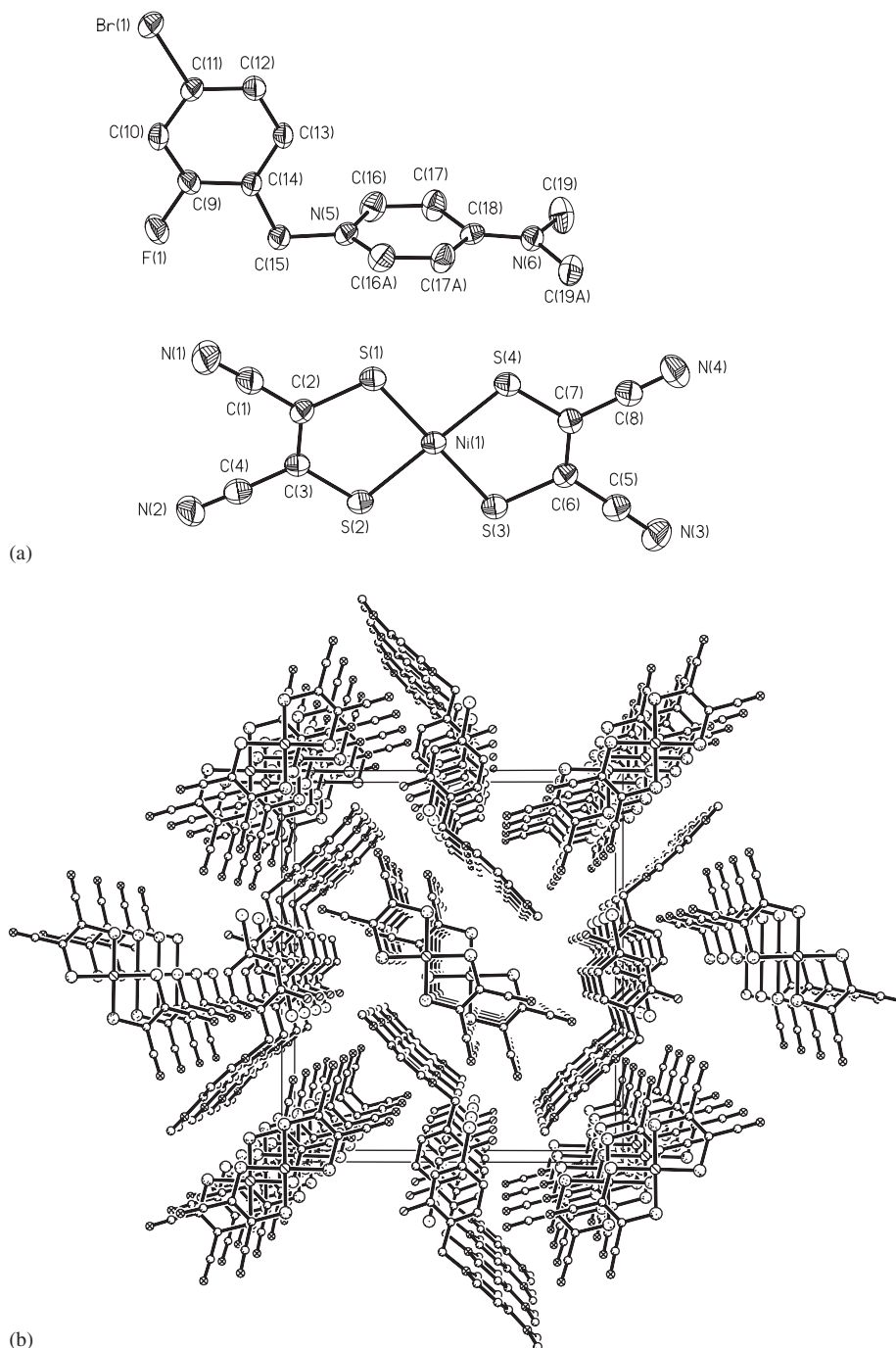


Fig. 1. (a) ORTEP plot (30% probability ellipsoids) showing the molecule structure of complex **1**. (b) The packing diagram of a unit cell for **1** as viewed along *b*-axis.

Ni ions is 4.227 Å and the nearest Ni...S and S...S contacts have 3.618 Å and 3.714 Å, respectively. Therefore, the Ni(III) ions form a quasi-one-dimensional zigzag uniform magnetic chain within a Ni(mnt)₂⁻ column through Ni...S, S...S, Ni...Ni, or π...π interactions (Fig. 2b). In a cationic column, the adjacent cations are stacked and form a quasi-one-dimensional column through weak π...π stacking interactions among the phenyl rings of neighboring cations (the contact distances of C(9)...C(11), C(10)...C(11), and C(10)...C(12) are 3.582, 3.631,

3.699 Å, respectively) (Fig. 3a). The most interesting fact in **1** is that the four columns of cations create a cubic-like large channel (extending along the crystallographic *b*-direction) (Fig. 3b) in which the Ni(mnt)₂⁻ columns are located (Fig. 1b). This geometry and stacking pattern for [BrFBzPyN(CH₃)₂]⁺ in **1** are significantly different from those of [BrFBzPyNH₂][Ni(mnt)₂] [16], and it is very rare in the conformation of cation for the Ni(mnt)₂⁻ complexes. Because the cationic columns mediate the anionic columns, the shortest intercolumn Ni...Ni distance of 12.373 Å is

Table 2
Selected bond parameters and intermolecular contacts for **1**

<i>Bond distances</i> (Å)	
Ni(1)–S(1)	2.139(1)
Ni(1)–S(2)	2.146(1)
Ni(1)–S(3)	2.138(1)
Ni(1)–S(4)	2.139(1)
S(1)–C(2)	1.726(4)
S(2)–C(3)	1.705(4)
S(3)–C(6)	1.713(5)
S(4)–C(7)	1.700(5)
<i>Bond angles</i> (°)	
S(1)–Ni(1)–S(2)	92.31(4)
S(1)–Ni(1)–S(4)	88.06(4)
S(2)–Ni(1)–S(3)	87.65(4)
S(3)–Ni(1)–S(4)	91.98(4)
<i>Intrachain distances</i> (Å)	
Ni...Ni (nearest separation)	4.227
Ni...S	3.681
S...S	3.714
<i>Interchain distances</i> (Å)	
Ni...Ni (nearest separation)	12.373

significantly greater than the intracolumn distance. As a result, **1** is a quasi-one-dimensional magnetic chain system from the point of view of the structure analysis. It is worth noting that two intermolecular hydrogen bonds between anions and cations were observed in the crystal structure of **1** as listed in Table 3. The anion–anion, anion–cation, and cation–cation contacts may play important roles in the crystal packing and stabilizing of **1**.

3.2. Magnetic property

The temperature dependence of the magnetic susceptibility for **1** is measured under an applied field of 2000 Oe in a temperature range 2–300 K. The plots of χ_m versus T and $\chi_m T$ versus T for **1** are shown in Fig. 4, where χ_m is the magnetic susceptibility per nickel atom corrected by the diamagnetic contribution. The overall magnetic behavior of **1** corresponds to a paramagnetic system with an antiferromagnetic coupling interaction. The $\chi_m T$ value at 300 K is only $0.250 \text{ emu K mol}^{-1}$, which is significantly

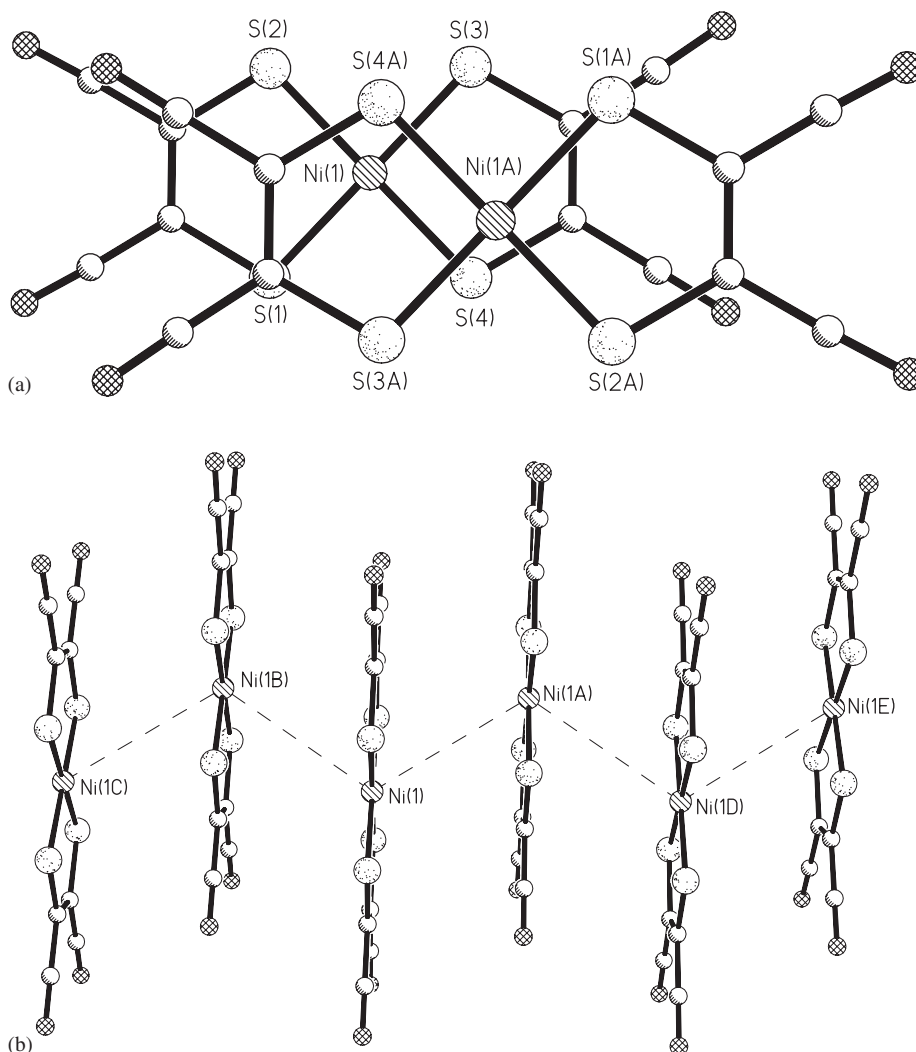


Fig. 2. (a) Mode of overlapping of $[\text{Ni}(\text{mnt})_2]^-$ anions for **1**. (b) The chain of $[\text{Ni}(\text{mnt})_2]^-$ anions with equal Ni...Ni distances viewing along the b -axis.

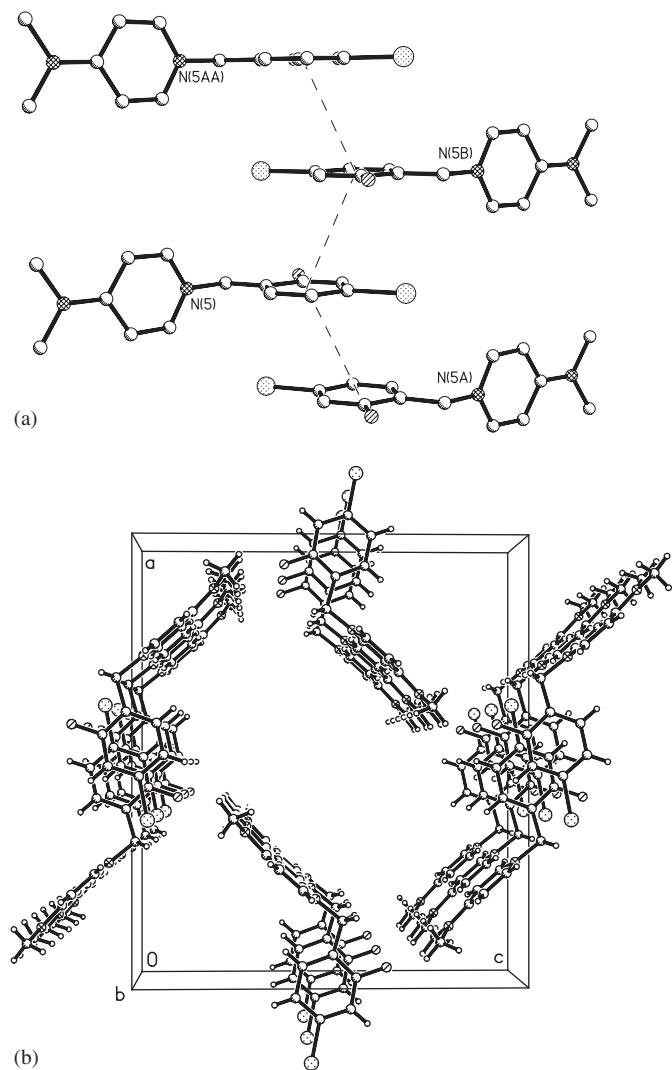


Fig. 3. (a) The 1D column of cations through weak $\pi \cdots \pi$ stacking interactions. (b) The cubic-like channel formed by four columns of cations along the crystallographic b -direction.

Table 3
Hydrogen bonds for **1** (Å and °)

D–H \cdots A	$d(\text{D–H})$	$d(\text{H}\cdots\text{A})$	$d(\text{D}\cdots\text{A})$	$\angle(\text{DHA})$
C(10)–H(10) \cdots N(2)#1	0.93	2.48	3.398(6)	169.0
C(19)–H(19C) \cdots N(1)#2	0.96	2.62	3.552(5)	165.0

Symmetry transformations used to generate equivalent atoms: #1 = $x+1/2, -y+1/2, -z+1/2$; #2 = $-x+3/2, -y, z+1/2$.

lower than the spin-only value expected for a $S = 1/2$ Ni(III) system ($0.375 \text{ emu K mol}^{-1}$). When the temperature decreases, the value of χ_m slightly decreases. Below around 200 K, the χ_m values decrease exponentially (Fig. 4a), indicating that **1** exhibits the characteristics of a spin gap system [20–23]. On increasing the temperature from 2 K back to 300 K, the same χ_m – T curves are obtained without hysteresis that indicates that complex **1** undergoes a reversible spin transition. The spin transition temperature is evaluated as the temperature at the maximum of the

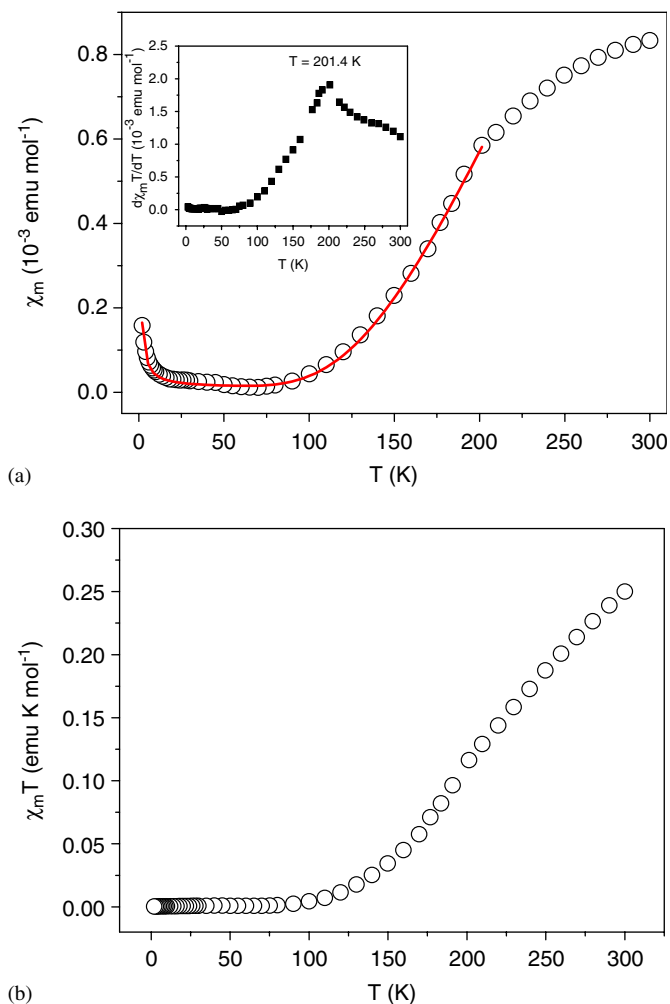


Fig. 4. (a) Plot of χ_m versus T for **1** (inset: plot of $d(\chi_m T)/dT$ versus T). The solid lines are reproduced from the theoretic calculations and detailed fitting procedure described in the text. (b) Plot of $\chi_m T$ versus T for **1**.

$d(\chi_m T)/dT$ derivative, that is, ~ 200 K for **1** (inset of Fig. 4a). It is very rare for Ni(mnt) $_2$ complexes with a spin-gap transition above 200 K [24,25]. The magnetic susceptibility for **1** may be simulated by the formula [26]:

$$\chi_m = \alpha \exp(-\Delta/k_b T)/T + C/T + \chi_0,$$

where α is a constant corresponding to the dispersion of excitation energy, Δ is the magnitude of the spin gap, k_b is the Boltzmann constant, C is a constant corresponding to the contribution of the magnetic impurity, χ_0 contributes from the core diamagnetism and the possible Van Vleck paramagnetism. A reasonable fit to the data within the range of 2–200 K for **1** are shown in Fig. 4(a) (the solid line), and the corresponding parameters are given as follows:

$\alpha = 4.88$, $\Delta/k_b = 755.31 \text{ K}$,
 $\chi_0 = 1.0 \times 10^{-5} \text{ emu mol}^{-1}$, $C = 3.1 \times 10^{-4} \text{ emu K mol}^{-1}$,
 and $R = 5.3 \times 10^{-6}$ (R is defined as $\sum((\chi_m^{\text{calcd}} - \chi_m^{\text{obsd}})^2 / (\chi_m^{\text{obsd}})^2)$). Magnetic impurity from the uncoupled Ni(mnt) $_2^-$ anions was estimated as 0.083%, based on the C value. The value of the parameter $2\Delta/k_b T_c$ (T_c is the transition temperature) is estimated to be 7.51 for **1**, which

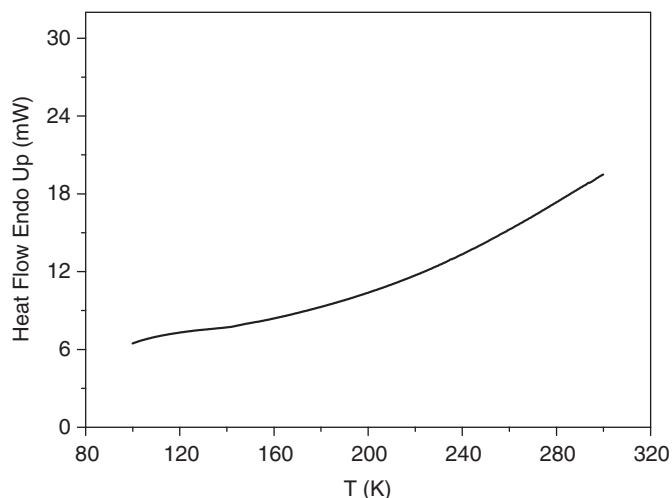


Fig. 5. DSC plot for **1**.

is higher than the ideal value of 3.53 derived from the BCS formula in a weak coupling regime. This result thus indicates that the spin transition is not a pure spin-Peierls transition [16], and are attributed to the cooperative interactions of Ni...S bonding, interplane repulsion of the $[\text{Ni}(\text{mnt})_2]^-$ anions, $\pi\cdots\pi$ stacking interactions between adjacent cations, spin–lattice interactions and spin–spin coupled interaction between nearest-neighbor anions [27–29].

Thermodynamic property of the phase transition for **1** was determined, and the power-compensated DSC trace for **1** from 100 to 300 K at a warming rate of 20 K min^{-1} is displayed in Fig. 5. No detectable endothermic peak in the corresponding temperature region was observed, indicating that the spin–gap transition of **1** is a second-order phase transition [11,13].

As for complexes containing $\text{Ni}(\text{mnt})_2^-$ anion, previous studies have shown that the magnetic coupling between $\text{Ni}(\text{mnt})_2^-$ anions is very sensitive to not only the overlap fashion of neighboring $\text{Ni}(\text{mnt})_2^-$ anions but also intermolecular contacts, and small structural change can result in large changes in the material properties of the $\text{Ni}(\text{mnt})_2^-$ complexes [3,4]. The theoretic studies using DFT have also revealed that magnetic exchange nature depend highly on the interplane distance (d) and the rotation angle (θ) [2]. Therefore, the magnetic behavior for **1** different from $[\text{BrFBzPyNH}_2][\text{Ni}(\text{mnt})_2]$ [16] may be understood as below, on the temperature being lowered, the non-uniform compression of the magnetic chain and slippage of the $\text{Ni}(\text{mnt})_2^-$ stack due to the anisotropic contraction of the crystal result in the magnetic-exchange constant changing and trigger a spin–gap transition.

4. Conclusion

In conclusion, we present a new molecular solid containing $\text{Ni}(\text{mnt})_2^-$ anion in which the anions in solid state form completely segregated uniform stacking columns

with the Ni...Ni distance being 4.227 \AA in the $\text{Ni}(\text{mnt})_2^-$ stacking column by intermolecular Ni...S, S...S, Ni...Ni, or $\pi\cdots\pi$ interactions at room temperature. The measurement of the temperature dependence of the magnetic susceptibility reveals that the title complex undergoes a spin–gap transition around 200 K, and exhibits antiferromagnetic interaction in the HT and spin gap in the LT. The spin–gap transition is a second-order phase transition as determined by DSC analyses.

5. Supplementary materials

Supplementary crystallographic data are available from the Cambridge Crystallographic Data Center, CCDC No. 601745. Copies of this information may be obtained free of charge from The Director, CCDC, 12 Union Road, Cambridge, CB2 1EZ, UK (fax: +44 1223 336033; deposit@ccdc.cam.ac.uk or <http://www.ccdc.cam.ac.uk>).

Acknowledgments

We thank financial support from the president's science foundation of South China Agricultural University (No. 2005K092).

References

- [1] N. Robertson, L. Cronin, *Coord. Chem. Rev.* 227 (2002) 93.
- [2] Z.P. Ni, X.M. Ren, J. Ma, J.L. Xie, C.L. Ni, Z.D. Chen, Q.J. Meng, *J. Am. Chem. Soc.* 127 (2005) 143301.
- [3] J. Nishijo, E. Ogura, J. Yamaura, A. Miyazaki, T. Enoki, T. Takano, Y. Kuwatani, M. Iyoda, *Solid State Commun.* 116 (2000) 661.
- [4] N. Robertson, C. bergemann, H. Becher, P. Agarwal, S.R. Julian, R.H. Friend, N.J. Hatton, A.E. Underhill, A. Kobayashi, *J. Mater. Chem.* 9 (1999) 1713.
- [5] A.E. Pullen, C. Faulmann, K.I. Pokhodnya, P. Cassoux, M. Tokumoto, *Inorg. Chem.* 37 (1998) 6714.
- [6] M. Urichi, K. Yakushi, Y. Yamashita, J. Qin, *J. Mater. Chem.* 8 (1998) 141.
- [7] J.F. Weiher, L.R. Melby, R.E. Benson, *J. Am. Chem. Soc.* 86 (1964) 4329.
- [8] P.I. Clemenson, A.E. Underhill, M.B. Hursthouse, R.L. Short, *J. Chem. Soc. Dalton Trans.* (1988) 1689.
- [9] A.T. Coomber, D. Beljonne, R.H. Friend, J.L. Brédas, A. Charlton, N. Robertson, A.E. Underhill, M. Kurmoo, P. Day, *Nature* 380 (1996) 144.
- [10] J.L. Xie, X.M. Ren, Y. Song, Y. Zou, Q.J. Meng, *J. Chem. Soc. Dalton Trans.* (2002) 2868.
- [11] X.M. Ren, Q.J. Meng, Y. Song, C.S. Lu, C.J. Hu, *Inorg. Chem.* 41 (2002) 5686.
- [12] J.L. Xie, X.M. Ren, S. Gao, W.W. Zhang, Y.Z. Li, C.S. Lu, C.L. Ni, W.L. Liu, Q.J. Meng, Y.G. Yao, *Eur. J. Inorg. Chem.* (2003) 2393.
- [13] J.L. Xie, X.M. Ren, C. He, Y. Song, Q.J. Meng, R.K. Kremer, Y.G. Yao, *Chem. Phys. Lett.* 369 (2003) 41.
- [14] X.M. Ren, Q.J. Meng, Y. Song, C.L. Lu, C.J. Hu, X.Y. Chen, Z.L. Xue, *Inorg. Chem.* 41 (2002) 5931.
- [15] J.L. Xie, X.M. Ren, Y. Song, W.W. Zhang, W.L. Liu, C. He, Q.J. Meng, *Chem. Commun.* (2002) 2346.
- [16] C.L. Ni, D.B. Dang, Y. Song, S. Gao, Y.Z. Li, Z.P. Ni, Z.F. Tian, L.L. Wen, Q.J. Meng, *Chem. Phys. Lett.* 396 (2004) 353.
- [17] S.B. Bulgarevich, D.V. Bren, D.Y. Movshovic, P. Finocchiaro, S. Failla, *J. Mol. Struct.* 317 (1994) 147.
- [18] A. Davison, R.H. Holm, *Inorg. Synth.* 10 (1967) 8.

- [19] G.M. Sheldrick, SHELXTL, Structure Determination Software Programs, Version 5.10. Bruker Analytical X-ray Systems Inc. Madison, Wisconsin, USA, 1997.
- [20] Y. Fujii, T. Goto, W. Fujita, K. Awaga, *Physica B* 329–333 (2003) 973.
- [21] C. Yasuda, S. Todo, M. Matsumoto, H. Takayama, *J. Phys. Chem. Solids* 63 (2002) 1607.
- [22] S. Nishihara, T. Akutagawa, T. Hasegawa, T. Nakamura, *Chem. Comm.* (2002) 408.
- [23] S. Nishihara, T. Akutagawa, T. Hasegawa, S. Fujiyama, T. Nakamura, *J. Solid State Chem.* 168 (2002) 661.
- [24] C.L. Ni, Y.Z. Li, D.B. Dang, Z.P. Ni, Z.F. Tian, Z.R. Yuan, Q.J. Meng, *Inorg. Chem. Commun.* 8 (2005) 105.
- [25] D.B. Dang, C.L. Ni, Y. Bai, Z.F. Tian, Z.P. Ni, L.L. Wen, Q.J. Meng, S. Gao, *Chem. Lett.* 5 (2005) 680.
- [26] L.C. Isett, D.M. Rosso, G.L. Bottger, *Phys. Rev. B* 22 (1980) 4739.
- [27] S. Alvarez, R. Vicente, R. Hoffman, *J. Am. Chem. Soc.* 107 (1985) 6253.
- [28] E. Pytte, *Phys. Rev. B* 10 (1974) 4637.
- [29] M.E. Itkis, X. Chi, A.W. Cordes, R.C. Haddon, *Science* 296 (2002) 1443.